Inorganic Chemistry

Article

pubs.acs.org/IC

DNA Condensing Effects and Sequence Selectivity of DNA Binding of Antitumor Noncovalent Polynuclear Platinum Complexes

Jaroslav Malina,[†] Nicholas P. Farrell,[‡] and Viktor Brabec*[,†]

[†]Institute of Biophysics, Academy of Sciences of the Czech Republic, v.v.i., Kralovopolska 135, CZ-61265 Brno, Czech Republic

[‡]Department of Chemistry, Virginia Commonwealth University, Richmond, Virginia 23284-2006, United States

Supporting Information

ABSTRACT: The noncovalent analogues of antitumor polynuclear platinum complexes represent a structurally discrete class of platinum drugs. Their chemical and biological properties differ significantly from those of most platinum chemotherapeutics, which bind to DNA in a covalent manner by formation of Pt-DNA adducts. In spite of the fact that these noncovalent polynuclear platinum complexes contain no leaving groups, they have been shown to bind to DNA with high affinity. We report here on the DNA condensation properties of a series of noncovalent analogues of antitumor polynuclear platinum complexes described by biophysical and biochemical methods. The results demonstrate that these polynuclear platinum compounds are capable of inducing DNA condensation at more than 1 order of magnitude lower concentrations than conventional spermine. Atomic force microscopy studies of DNA condensation confined to a mica substrate have revealed that the DNA morphologies become more compact with increasing concentration of the platinum complexes. Moreover, we also found that the noncovalent polynuclear platinum complex $[\{Pt(NH_3)_3\}_2$-μ-$\{trans$-$Pt(NH_3)_2(NH_2(CH_2)_6NH_2)_2\}]^{6+}$ (TriplatinNC-A) binds to DNA in a sequence-dependent manner, namely, to A/T-rich sequences and A-tract regions, and that noncovalent polynuclear platinum complexes protect DNA from enzymatic cleavage by DNase I. The results suggest that mechanisms of antitumor and cytotoxic activities of these complexes may be associated with their unique ability to condense DNA along with their sequence-specific DNA binding. Owing to their high cellular accumulation, it is also reasonable to suggest that their mechanism of action is based on the competition with naturally occurring DNA condensing agents, such as polyamines spermine, spermidine, and putrescine, for intracellular binding sites, resulting in the disturbance of the correct binding of regulatory proteins initiating the onset of apoptosis.

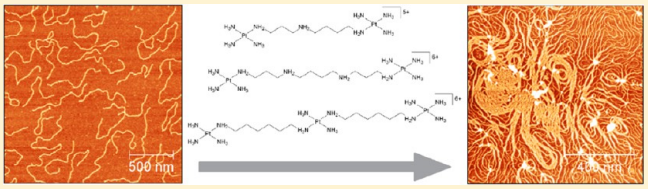

INTRODUCTION

The length of a stretched single DNA molecule may be up to several dozens of centimeters depending on the organism, which is in eukaryotes orderly packed to be readily accessible inside the micrometer-sized nucleus. DNA molecules can be compacted by monomolecular condensation or multimolecular aggregation. One way to induce DNA condensation in vitro is to induce attractive interactions between the DNA segments. This possibility can be accomplished by inducing attractive interactions between the DNA segments by multivalent cationic charged ligands, such as multivalent metal ions, inorganic cations, polyamines, protamines, peptides, lipids, liposomes, and proteins.[1] Mechanistic details of DNA condensation are essential for its functioning in the process of gene regulation in living systems. In addition, DNA condensation has many potential applications in medicine and biotechnology.[2] Therefore, studies of DNA condensation induced by cationic charged ligands of biological (pharmacological) significance are of great interest.

The noncovalent polynuclear platinum complexes $[\{Pt(NH_3)_3\}_2$-μ-$Y]^{n+}$ [Y = spermidine, spermine or $\{trans$-$Pt(NH_3)_2(NH_2(CH_2)_6NH_2)_2\}$; Figure 1] have been synthesized[3] as analogues of antitumor polynuclear platinum complexes, by replacing the chloride leaving groups with ammonia. Polynuclear platinum compounds represent a very promising group of anticancer platinum drugs that significantly differ in DNA binding and antitumor activity from their mononuclear counterparts, such as cisplatin and its analogues.[4,5] The trinuclear $[\{trans$-$PtCl(NH_3)_2\}_2(\mu$-$trans$-$Pt(NH_3)_2\{NH_2(CH_2)_6NH_2\}_2)]^{4+}$ (BBR3464) has even undergone phase I and II human clinical trials, but it has not advanced to full use.[6−8] Interestingly, it has been shown using atomic force microscopy (AFM) that the molecules of circular supercoiled pBR322 plasmid get compacted after treatment with BBR3464 in cell-free media.[9]

The unique biological properties of polynuclear complexes have been attributed not only to coordinative binding to DNA base residues but also to the linker interactions with DNA through electrostatic and hydrogen-bonding effects. It has been shown that the presence of charge in the linker, either as the central tetraamine unit of a trinuclear compound or through a polyamine linker such as spermidine or spermine in dinuclear complexes, greatly enhances the cytotoxicity and antitumor activity.[10,11] Much attention has been paid to the preassociation of the polynuclear platinum complexes on DNA prior to

Received: November 7, 2013
Published: January 16, 2014

   dx.doi.org/10.1021/ic402796k | Inorg. Chem. 2014, 53, 1662−1671

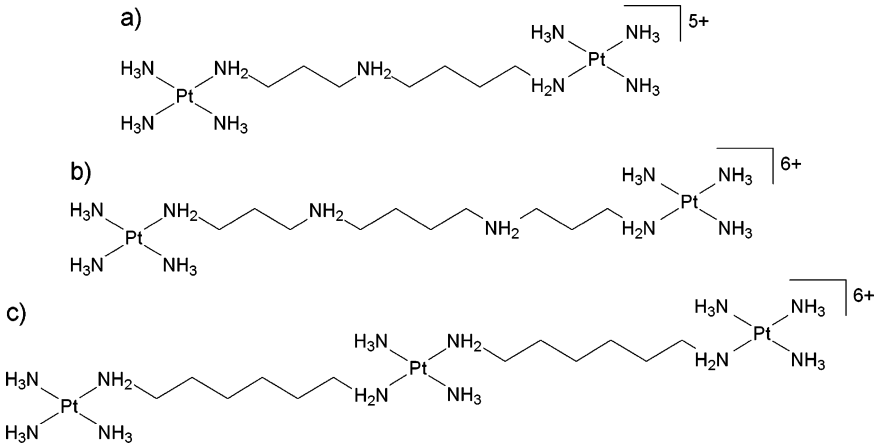

Figure 1. Chemical structures of the di- and trinuclear linear platinum polyamine compounds: (a) $[\{Pt(NH_3)_3\}_2$-μ-spermidine$]^{5+}$ (**I**); (b) $[\{Pt(NH_3)_3\}_2$-μ-spermine$]^{6+}$ (**II**); (c) $[\{Pt(NH_3)_3\}_2$-μ-{*trans*-$Pt(NH_3)_2(NH_2(CH_2)_6NH_2)_2\}]^{6+}$ (**III**, TriplatinNC-A).

coordination bond formation.[12−14] Such interactions may significantly affect the kinetics of cross-link formation and the local structure of the cross-links formed.[13,15]

The noncovalent analogues of polynuclear platinum complexes were first developed as model compounds with the intention of further investigating charge effects on preassociation and on DNA conformational changes induced by di- and trinuclear platinum complexes in the absence of coordinative Pt-DNA bond formation. These noncovalent analogues have been shown[3] to bind to DNA with high affinity, stabilize it, and induce B → Z and B → A transitions in susceptible sequences at concentrations lower than those required by cobalt hexammine, a DNA condensing agent capable of condensing DNA from very dilute aqueous solutions.[16] Interestingly, these noncovalent platinum compounds have exhibited cytotoxicity in human ovarian cancer cells.[3] In particular, $[\{Pt(NH_3)_3\}_2$-μ-{*trans*-$Pt(NH_3)_2(NH_2(CH_2)_6NH_2)_2\}]^{6+}$, the noncovalent congener of BBR3464 (**III**, TriplatinNC-A; Figure 1c), displayed cytotoxic activity in several ovarian carcinoma cancer cell lines and induced caspase-dependent apoptosis in both primary mast cells and transformed mastocytomas,[17,18] which suggests compounds such as **III** and its derivatives as a possible new class of antitumor agents in their own right.

The mechanism of cytotoxic activity of **III** is not known. On the other hand, it has been shown that the cellular uptake of **III** is much greater than that of neutral cisplatin as well as other multinuclear platinum compounds[17,18] and that the chemical modifications increasing the charge of these platinum linear cations result in significantly enhanced cellular accumulation and consequently enhanced cytotoxicity.[17,18] The dependence of the antitumor and cytotoxic activity on the charge has been previously described for synthetic polyamine analogues.[19,20] Moreover, all synthetic polyamine analogues are efficient inducers of DNA condensation in a cell-free system, and their cytotoxicities generally parallel their abilities to condense DNA.[20] The mechanism of antitumor activity of polyamine analogues is not fully understood. However, it is believed that it is based on binding to nucleic acids, in particular on competition with natural polyamines for intracellular binding sites but with altered function. If we consider the similarity in the chemical structures between polyamines and noncovalent multinuclear platinum compounds and their high affinity for DNA, it seems reasonable to hypothesize that their mechanisms of action might be related.

In the present paper, we report on the DNA condensation properties in cell-free media of a series of noncovalent analogues of antitumor polynuclear platinum complexes (Figure 1). Moreover, because the sequence selectivity of DNA binding is a crucial underlying factor mediating biological effects of DNA binders by indirect readout, the sequence selectivity of noncovalent analogues of polynuclear platinum complexes has been evaluated as well.

RESULTS AND DISCUSSION

Static Light Scattering. To determine the efficacy of noncovalent polynuclear platinum compounds to condense DNA, we employed a total intensity light scattering assay described by Vijayanathan et al.[21] This method is based on the measurement of the intensity of light scattered by the diluted DNA solution at 90°. The scattered light intensity is low in the absence of or at low concentration of the condensing agent. However, a marked increase in the intensity of the scattered light appears at a critical concentration of the condensing agent because of the formation of condensed DNA particles. The increase in the intensity of the scattered light is concentration-dependent up to a certain concentration of the condensing agent, and then it levels off. The efficacy of various condensing agents to induce DNA condensation can be quantified by determining the EC_{50} value, which is the concentration of a condensing agent at the midpoint of DNA condensation.

Table 1 shows EC_{50} values determined for spermidine, spermine, and **I**−**III** in the presence of 10 mM Na^+. As expected, spermidine was the least efficient in calf thymus (CT) DNA condensation and had the highest EC_{50} value (30 ± 3 μM). Spermine proved to be ∼8-fold more efficient than spermidine having the EC_{50} value of 4.1 ± 0.5 μM, which is in an excellent agreement with the EC_{50} value published previously.[21] The EC_{50} values of the polynuclear platinum complexes were even ∼110−150-fold and ∼15−20-fold lower than that of spermidine and spermine, respectively, and comparable to EC_{50} values obtained for synthetic polyamine derivatives with 6+ charge.[22]

Compound **III** was the most efficient with a EC_{50} value of 0.20 ± 0.01 μM, while compounds **I** and **II** had EC_{50} values of 0.27 ± 0.02 and 0.25 ± 0.02 μM, respectively. Unsurprisingly, compound **I** was less effective in inducing DNA condensation

dx.doi.org/10.1021/ic402796k | Inorg. Chem. 2014, 53, 1662−1671

Table 1. EC_{50} Values of Polyamines and Platinum Compounds[a]

compound	EC_{50} (μM)
spermidine	30 ± 3
spermine	4.1 ± 0.5
I	0.27 ± 0.02*,#
II	0.25 ± 0.02*,#
III	0.20 ± 0.01*

[a]All measurements were conducted in a 10 mM sodium cacodylate buffer, pH 7.2, at 25 °C. EC_{50} values were determined by plotting the scattered light intensity against the concentration of condensing agents. Data are mean ± SD of three separate measurements. The symbol * denotes a significant difference ($p < 0.005$) from spermidine and spermine, and the symbol # denotes a significant difference ($p < 0.005$) between **I** or **II** and **III**. For other details, see the text.

than its two counterparts because it has a lower charge of 5+. On the other hand, the difference between **II** and **III** possessing the same charge 6+ indicates that not only the overall charge but also the structural properties play an important role in the condensing activity of these compounds. It has been shown that the efficiency of the condensing agent is greatly influenced by the distance between the charges in multivalent cations and is the best if there is a geometrical fit between DNA phosphates and the multication charges.[23] It might be the key for the explanation of better condensing activity of **III** because the crystal structure of the B-DNA Dickerson–Drew dodecamer bound to **III**[24] revealed that **III** binds with high selectivity to phosphate oxygen atoms and thus associates with the backbone. The three PtN_4 coordination units form bidentate N···O···N complexes with OP atoms, in a motif called the "phosphate clamp". This recently discovered unique binding mode[25] is a general feature of DNA complexes of PtN_4 containing nonreactive polynuclear platinum complexes. The backbone selective binding of **III** and the close proximity of the Pt^{2+} centers from the negatively charged phosphates due to the formation of phosphate clamps may contribute to the increased condensing effectivity of compound **III**.

Flow Linear Dichroism (LD). The condensation of CT DNA by the noncovalent analogues of polynuclear platinum complexes was investigated using LD spectroscopy as well. The LD spectra (Figure 2a–c) show that the DNA band at 260 nm subsequently disappears with increasing concentration of the platinum complexes {decreasing mixing ratios ([DNA base]:[Pt complex])}. This is because the orientation of the DNA in the flow cell is attenuated when long stretches of DNA disappear as the DNA becomes condensed.[26,27] In accordance with the results of light scattering (Table 1), compounds **II** and **III** were more efficient in DNA condensation than **I** (Figure 2d).

Absorption UV/Vis Spectrophotometry. We have employed a spectrophotometric technique to follow changes in the state of condensation/aggregation of the DNA complexes upon binding of the noncovalent analogues of polynuclear platinum complexes. The turbidity of the solutions was determined spectrophotometrically by monitoring the absorbance of CT DNA at 350 nm. Figure S1 in the Supporting Information (SI) illustrates the effect of adding **I**, **II**, or **III** to the CT DNA on the absorbance at 350 nm, which starts to rise, indicating the onset of turbidity characteristic of the condensation process.[28] The turbidity increases as the concentration of the platinum complexes is increased (Figure 3a) and levels off upon the addition of **II** or **III** at a

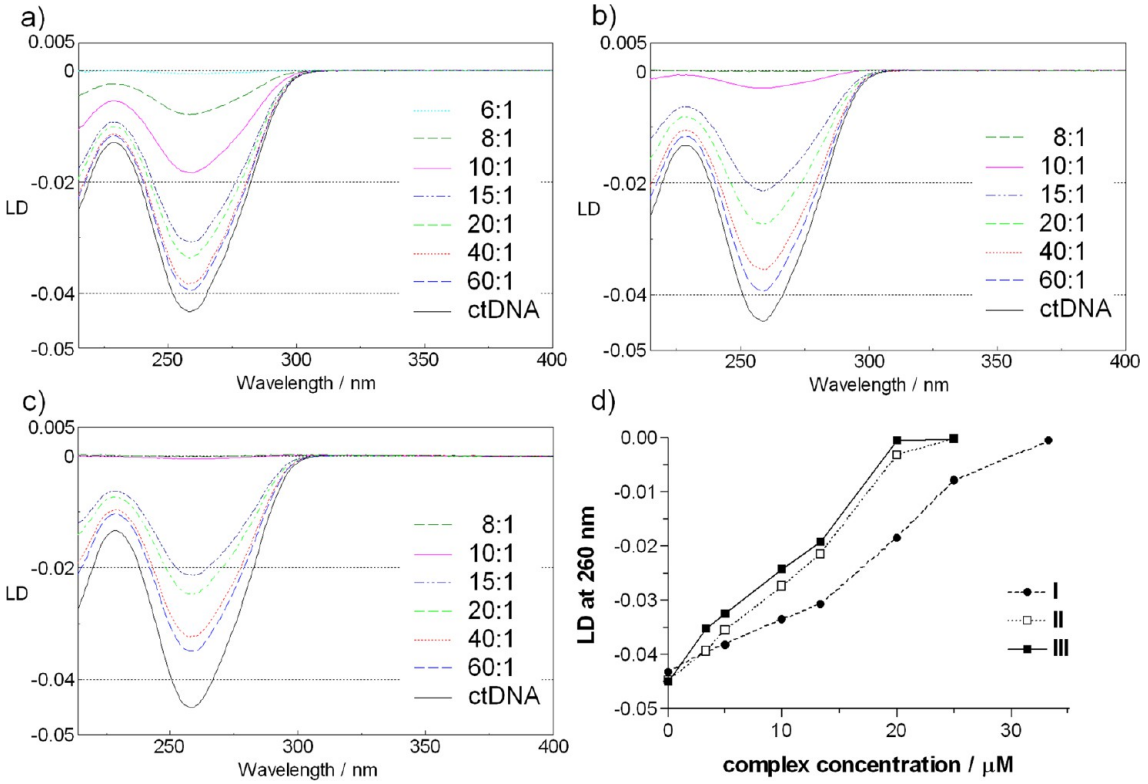

Figure 2. LD spectra of free CT DNA (2×10^{-4} M; 10 mM NaCl, 1 mM sodium cacodylate, pH 7.0, 25 °C) and in the presence of **I** (a), **II** (b), or **III** (c). Mixing ratios ([DNA base]:[Pt complex]) are indicated in the figure. (d) LD signal at 260 nm versus the concentration of **I** (●), **II** (□), and **III** (■) in the presence of CT DNA.

dx.doi.org/10.1021/ic402796k | Inorg. Chem. 2014, 53, 1662–1671

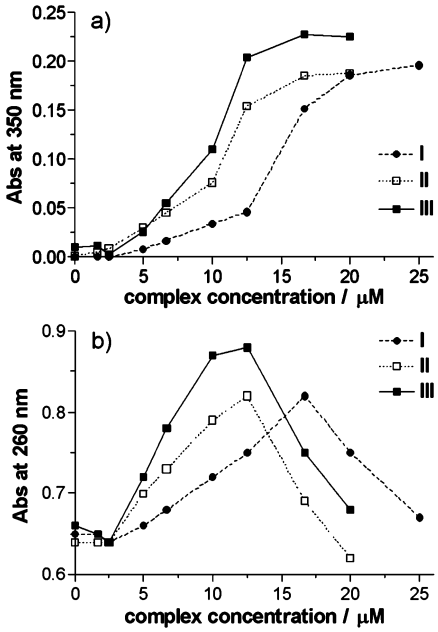

Figure 3. Absorption of CT DNA (1×10^{-4} M; 10 mM NaCl, 1 mM sodium cacodylate, pH 7.0, 25 °C) in the presence of **I**, **II**, or **III** at 350 nm (a) and 260 nm (b) versus the concentration of **I** (●), **II** (□), and **III** (■) in the presence of CT DNA. Note the sudden drop in the absorption value at 260 nm close to the concentration of ~15 μM **II** or **III** or at the concentration of ~18 μM **I** (due to the formation of aggregates) and the leveling off at 350 nm at the same points, implying enhanced turbidity.

concentration of ~15 μM or upon the addition of **I** at a concentration of ~18 μM. We diagnosed DNA modified by the noncovalent analogues of polynuclear platinum complexes also by monitoring the absorbance of DNA at 260 nm and 25 °C. The absorbance at 260 nm increases as the concentration of the platinum complexes is increased (Figure 3b), mainly because of the increase of turbidity, and started to decrease upon the addition of **II** or **III** at a concentration of ~15 μM or upon the addition of **I** at a concentration of ~18 μM apparently because of aggregation[29] because the aggregated particles do not absorb or absorb much less at 260 nm.[30]

Gel Retardation Assay. The ability of noncovalent analogues of polynuclear platinum complexes to condense DNA was further assessed by gel retardation assay.[31] Retardation of the DNA mobility in the gel upon treatment with condensing agents indicates neutralization of the negative charge on the DNA as well as formation of large-size DNA complexes.[32,33] The results (Figure 4) demonstrate that all noncovalent analogues of polynuclear platinum complexes efficiently condense negatively supercoiled plasmid DNA. When their concentration exceeded 6 μM, no bands corresponding to the free DNA could be detected in the gel. This is much lower concentration in comparison with other recently developed condensing agents such as macrocyclic polyamines[31] or a tetranuclear nickel(II) complex.[32] The differences among **I**–**III** were small (Figure 4); however, in accordance with the results of light scattering experiments (Table 1), complex **III** exhibited the highest condensing activity, with most DNA confined to the gel loading well when the concentration of **III** reached 6 μM (Figure 4c, lane 3).

Reversibility of DNA Condensation. It is known that the DNA condensation induced by multivalent cations is a

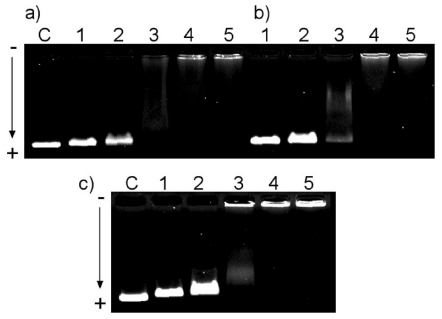

Figure 4. Effect of **I** (a), **II** (b), and **III** (c) on the migration of the negatively supercoiled plasmid pSP73 in the native agarose gel at 25 °C. Lane C: control, nonmodified plasmid DNA. Lanes 1–5: plasmid DNA in the presence of 1.5, 3.0, 6.0, 9.0, and 12.0 μM platinum compounds, respectively. The DNA concentration in the samples was 30 μM.

reversible process. The unfolding of the compact DNA can be achieved by various means such as by the addition of a high concentration of monovalent cations (NaCl)[34] as a result of the electrostatic competition between multivalent and monovalent cations with the phosphate backbone of DNA. To examine the reversibility of DNA condensation by platinum compounds, we treated samples containing DNA condensed by noncovalent analogues of polynuclear platinum complexes with a high concentration of NaCl (0.65 M) and analyzed them on native agarose gel. As can be seen in Figure 5, the condensed plasmid

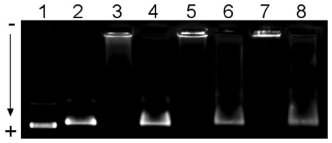

Figure 5. Effect of a high concentration of NaCl on the reversibility of the negatively supercoiled plasmid pSP73 condensation induced by noncovalent analogues of polynuclear platinum complexes in a Tris-HCl buffer (10 mM, pH 7.4) and at 25 °C. Lane 1: control, nonmodified DNA. Lane 2: nonmodified DNA treated with NaCl (0.65 M). Lane 3: DNA mixed with **I**. Lane 4: DNA mixed with **I** and then treated with NaCl (0.65 M). Lane 5: DNA mixed with **II**. Lane 6: DNA mixed with **II** and then treated with NaCl (0.65 M). Lane 7: DNA mixed with **III**. Lane 8: DNA mixed with **III** and then treated with NaCl (0.65 M). The concentrations of DNA and the platinum compounds were 30 and 12 μM, respectively.

pSP73 was released after being treated with 0.65 M NaCl, which confirms that the DNA condensation induced by **I**–**III** is reversible. We tested several lower concentrations of NaCl, but concentrations below 600 mM were not sufficient to completely restore condensed DNA to the relaxed form.

AFM Imaging. In order to determine and compare the morphology of the DNA condensates induced by platinum compounds **I**–**III**, we used an atomic force microscope with tapping mode in air. Figure S2 in the SI shows images of the linearized plasmid pSP73 (linearized by *Nde* I restriction endonuclease, which cuts only once within this plasmid) in the presence of increasing concentrations of spermidine (Figures S2A–C in the SI) and spermine (Figure S2D–F in the SI). At low concentrations of spermidine (below ~400 μM), the DNA molecules were linear with rare inter- or intramolecular contacts. As the concentration was getting close to 400 μM, we observed the formation of intramolecular loops (Figure S2A

dx.doi.org/10.1021/ic402796k | *Inorg. Chem.* 2014, 53, 1662–1671

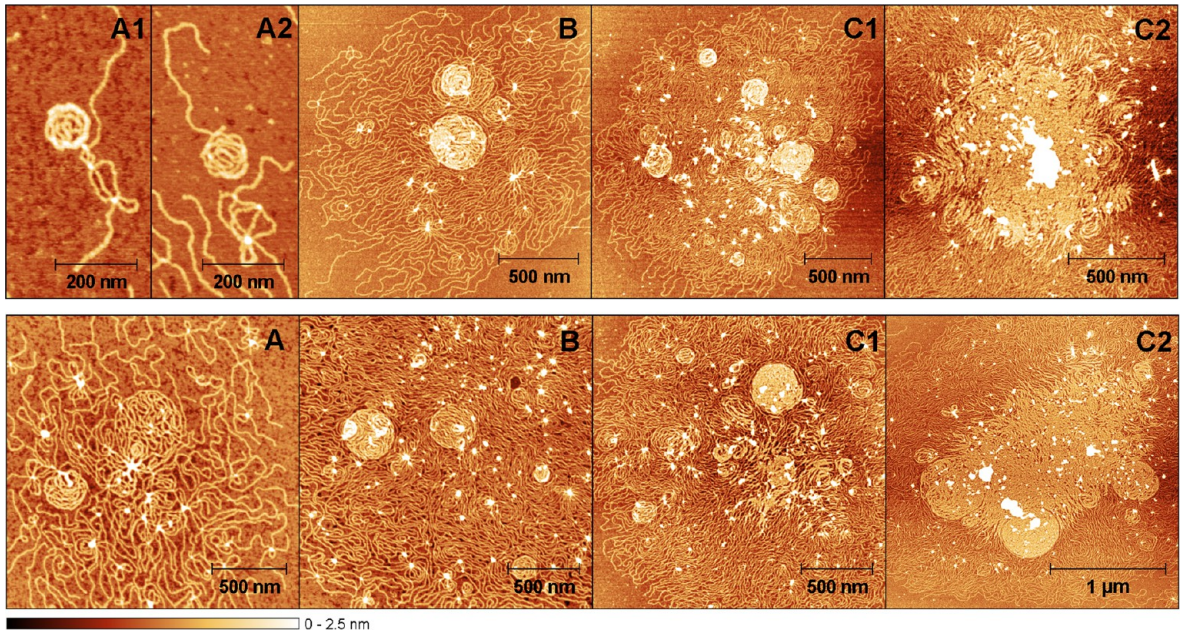

Figure 6. Representative AFM images of linearized plasmid pSP73 in the presence of (top panels A–C) complex **I** at 6.25, 12.5, and 25 μM concentrations, respectively, and (bottom panels A–C) complex **II** at 6.25, 25, and 50 μM concentrations, respectively.

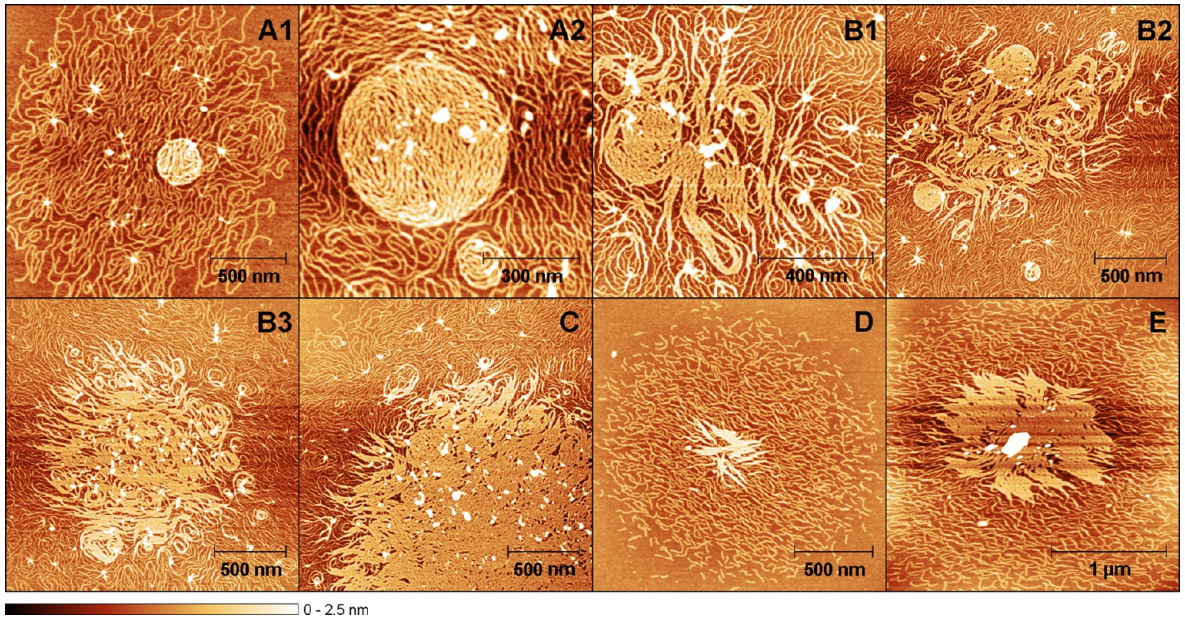

Figure 7. (A–C) Representative AFM images of linearized plasmid pSP73 in the presence of complex **III** at 6.25, 12.5, and 25 μM concentrations, respectively. (D and E) Representative AFM images of a 158 bp *Hind* III/*Nde* I restriction fragment of the plasmid pSP73 in the presence of complex **III** at 25 and 50 μM concentrations, respectively.

in the SI). With increasing concentration of spermidine, the initially individual-looped molecules started to cross over and formed multimolecular "flower"-shaped structures (Figure S2B in the SI). A further increase of the spermidine concentration led to the formation of very large (>500 nm) multimolecular aggregates (Figure S2C in the SI) reminiscent of flowers. Our images of DNA condensates formed by spermidine are quite similar to those obtained previously.[35] The fact that we did not observe the formation of disklike aggregates reported by Fang and Hoh[35] may be caused by the different buffer that we used and by the slightly different approach to prepare the samples including rinsing of the samples with water prior to drying.

The DNA condensates induced by spermine look different from those induced by spermidine (Figure S2D–F in the SI). Spermine proved to be much more efficient in DNA condensation than spermidine. The concentration of spermine, sufficient to observe the formation of massive multimolecular DNA aggregates (>3 μm in diameter; Figure S2F in the SI), was approximately 5-fold lower than that of spermidine. Similarly to spermidine, the DNA molecules in the presence of low concentrations of spermine were rarely in contact with each other and formed rather intramolecular loops. At 50 μM spermine concentration, the DNA molecules started to form large intermolecular aggregates (Figure S2D1 in the SI) often

dx.doi.org/10.1021/ic402796k | *Inorg. Chem.* 2014, 53, 1662–1671

containing circular "disk"-like structures of various diameters (Figure S2D2 in the SI). The strands within the disks are thicker than double-stranded DNA molecules outside the disks, suggesting that the strands within the disk are composed of two or more closely associated DNA strands. With increasing concentration of spermine, the DNA aggregates become larger (Figures S2E,F in the SI), reaching diameters of several micrometers. These large complex structures contain disks as well as flowerlike structures.

Compound **I** is based on spermidine; however, its charge of 5+ is significantly higher than 3+ of the spermidine itself. This is possibly one of the main reasons why the images of DNA condensates formed in the presence of **I** resemble rather those formed by spermine (4+). At low concentrations (~6.25 μM), complex **I** induced the formation of intra- and intermolecular loops, multimolecular flowerlike structures, and also small DNA clews composed of a few closely associated DNA molecules (Figure 6, top panels A1 and A2). At higher concentrations, predominantly large intermolecular aggregates containing flower- and disklike structures (Figure 6, top panel B) were formed. The size of the DNA condensates grew with increasing concentration of **I**, and at 50 μM, we could observe very large DNA condensates having several micrometers diameter (Figure 6, top panel C). The DNA molecules inside these condensates become so densely arranged that they form flat monolayers where individual molecules cannot be resolved (Figure 6, top panel C2). Such layers then often serve as a new surface for additional condensation (Figure 6, top panel C2).

In accordance with the results of light scattering (Table 1) and gel retardation (Figure 4) experiments, compounds **II** and **III** were more efficient in DNA condensation than **I**, in particular owing to their higher charge of 6+. Figure 6 (bottom panel A) shows typical DNA aggregates formed in the presence of **II** at 6.25 μM concentration. The DNA molecules are quite loosely associated, and multimolecular loops, flowerlike structures, and the formation of disklike structures from the set of loops of multimolecular flowers can be seen. Figure 6 (bottom panel B) shows how the DNA aggregates get bigger with increasing concentration of **II** and the DNA molecules become more tightly associated. The DNA aggregate contains several disklike structures of various sizes. At a 25 μM concentration of **II** (the highest concentration examined), we could observe large-sized DNA condensates (Figure 6, bottom panel C), and similarly to **I**, the formation of monolayers of densely packed DNA molecules (Figure 6, bottom panel C2).

Our previous experiments have revealed (Table 1 and Figures 2–4) that the potency of **III** to condense DNA was the highest among all tested noncovalent analogues of polynuclear platinum complexes. Indeed, the AFM images confirm that complex **III** was slightly more efficient than **II** in inducing DNA condensation. Figure 7A represents images of DNA condensates in the presence of **III** at 6.25 μM concentration. The formation of typical disklike structures within the DNA aggregates can be seen (Figure 7A2). In contrast to **II**, compound **III** tends at higher concentrations to form more compact condensation patterns and toroidal structures (Figure 7B). Figure 7C shows a large monolayer of densely packed DNA molecules within an enormous DNA condensate generated in the presence of **III** at 25 μM concentration. We also investigated the effect of **III** on the condensation of a 158 base pair (bp) *Hind* III/*Nde* I restriction fragment of the plasmid pSP73 used for DNase I footprinting (vide infra). In the presence of low concentrations of **III** up to ~25 μM, we observed the formation of clusters of loosely associated DNA molecules rather than aggregates. As expected, we did not see any loops or strong bending because the length of the 158 bp fragment is very close to the persistence length (~50 nm). Parts D and E of Figure 7 show DNA aggregates induced by **III** at 25 and 50 μM concentrations, respectively. The formation of DNA monolayers in the centers of the aggregates that can in the latter case serve as a surface for further condensation can be seen. The concentration (in bp's) of the 158 bp fragment during these investigations was 4-fold lower (see the Experimental Section) than the concentration of linearized plasmid pSP73, which might be the reason why a slightly higher concentration of **III** was necessary to induce the formation of DNA aggregates. A shorter length of the fragment in comparison with the plasmid might also play a role.

EtBr Displacement. The competition assay based on the displacement of EtBr from a DNA double helix was employed to quantify the binding strengths of noncovalent analogues of polynuclear platinum complexes to CT DNA, and synthetic double-stranded DNA copolymers poly(dA-dT)$_2$ and poly(dG-dC)$_2$. The displacement of EtBr from all studied DNA was accompanied by a decrease in the fluorescence intensity measured at 595 nm. The apparent binding constants (K_{app}) were calculated from K_{EB}[EB] = K_{app}[drug], where [drug] is the concentration of the platinum complex at a 50% reduction of the fluorescence and K_{EB} is known.[36] The K_{app} values listed in Table 2 reveal that compounds **I** and **III** exhibit higher binding affinity for poly(dA-dT)$_2$ than for CT DNA and poly(dG-dC)$_2$, although the binding preference to poly(dA-dT)$_2$ for **I** is lower than that for **III**. Overall, compound **III** shows the highest binding affinity to all tested DNA.

Table 2. Apparent Binding Constants K_{app} ($\times 10^6$ M^{-1}) Determined at 25 °C[a]

compound	CT DNA	poly(dA-dT)$_2$	poly(dG-dC)$_2$
I	28 ± 3	34 ± 3	25 ± 2
II	34 ± 2	33 ± 3	33 ± 2
III	36 ± 2	50 ± 2	39 ± 1

[a]Data are mean ± SD of three separate measurements.

DNase I Footprinting. In order to obtain further information on the sequence-specific binding of noncovalent analogues of polynuclear platinum complexes to DNA, a DNase I footprinting experiment was performed (Figure 8). The 158 bp *Hind* III/*Nde* I restriction fragment of the plasmid pSP73 was treated with noncovalent analogues of polynuclear platinum complexes at various concentrations followed by partial cleavage by DNase I. Inspection of the gel shown in Figure 8a reveals that DNA cleavage at a 90 μM concentration of the platinum complex was completely inhibited by **II** and **III** (Figure 8a, lanes 4 and 7, respectively) and almost completely by **I** (Figure 8a, lane 1). Compound **III** strongly inhibited DNA cleavage even at 45 μM (Figure 8a, lane 8). A plausible explanation of this observation is that the inhibition was caused by DNA condensation induced by the platinum compounds protecting the DNA from cleavage by DNase I. The reversibility of DNA condensation induced by **I**–**III** is corroborated by unaltered intensities and positions of the bands corresponding to the full-length fragment (Figure 8a, lanes 1, 4, and 7, respectively), indicating that condensed DNA in the samples was fully released after precipitation and washing of the samples with ethanol. These observations are in

dx.doi.org/10.1021/ic402796k | Inorg. Chem. 2014, 53, 1662–1671

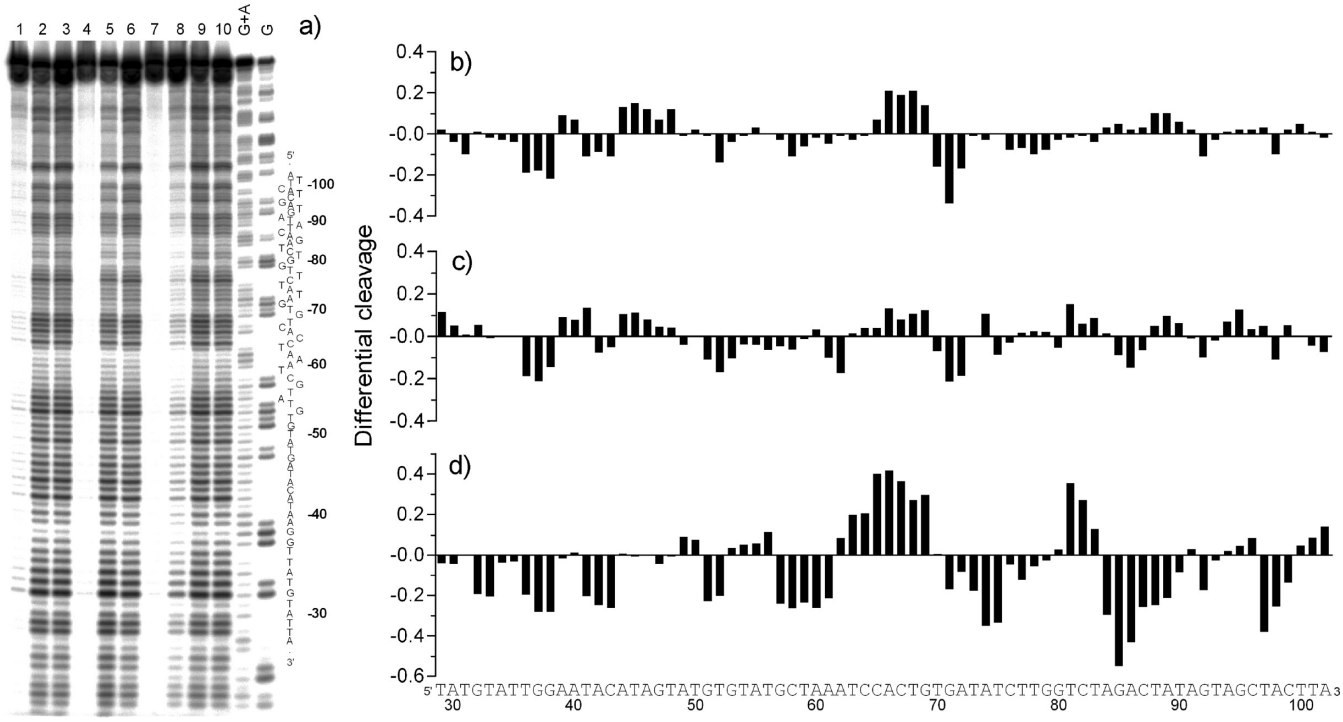

Figure 8. (a)Autoradiogram of a DNase I footprint of a 3′-end-labeled 158 bp *Hind* III/*Nde* I restriction fragment of the plasmid pSP73 in the presence of various concentrations of noncovalent analogues of polynuclear platinum complexes. Lanes 1−3: DNA mixed with complex **I** at 90, 45, and 22.5 μM concentrations, respectively. Lanes 4−6: DNA mixed with complex **II** at 90, 45, and 22.5 μM concentrations, respectively. Lanes 7−9: DNA mixed with complex **III** at 90, 45, and 22.5 μM concentrations, respectively. Lane 10: DNA in the absence of platinum complexes. Lanes G+A and G correspond to Maxam−Gilbert G+A and G ladders.

agreement with previous experiments investigating the DNA condensation properties of platinum complexes and showing that **III** was the most and **I** the least efficient in DNA condensation. No clear footprints in the remaining gel lanes not affected by DNA condensation that would indicate sequence specific binding can be seen. However, when the intensities of the bands from the lanes containing DNA treated with 45 μM **I** or **II** (Figure 8a, lanes 2 and 5, respectively) or 30 μM **III** (the gel is not shown) were evaluated by densitometry, some patterns of protection and enhancement can be observed in the resulting differential cleavage plots (Figure 8b−d). The concentrations 45 μM for **I** or **II** and 30 μM for **III** were chosen for analysis as the highest concentrations not affected by DNA condensation and subsequent inhibition of cleavage by DNase I. Complexes **I** and **II** (Figures 8b,c) exhibit only weak patterns of protection and enhancement. The patterns induced by **III** (Figure 8d) are not very distinct either but stronger than those obtained for **I** or **II**. There are three sites protected by **III** extending over 5−6 bp's, around positions 59, 74, and 86, and another three sites extending over 3 bp's, around positions 37, 42, and 98. If we consider a 3′ shift of about 2−3 bp's due to the bias introduced by DNase I upon DNA cleavage,[37] we obtain binding sites 5′-AAG (40), 5′-TAC (45), 5′-TAAAT (63), 5′-TCTAT (77), 5′-ATATCA (91), and 5′-TTC (101) containing mainly A/T-rich sequences and A-tract regions, implying a potential preference for the A−T sequence. A similar binding preference has been described previously for natural polyamines, such as putrescine, spermidine, and spermine,[38] although at much higher millimolar concentrations of these compounds.

The nucleotide sequence of the fragment is shown on the right side of the gel, and numbers refer to the sequence shown in the corresponding differential cleavage plots in Figure 8b−d. The temperature at which these experiments were conducted was 25 °C. Differential cleavage plots comparing the susceptibility of the 158 bp *Hind* III/*Nde* I restriction fragment of the plasmid pSP73 in the presence of **I** (b), **II** (c), and **III** (d) at 45, 45, and 30 μM concentrations, respectively. Vertical scales are in units of $\ln(f_c) - \ln(f_0)$, where f_c is the fractional cleavage at any bond in the presence of the platinum complex and f_0 is the fractional cleavage of the same bond in the control, given closely similar extents of overall digestion. Positive values indicate enhancement and negative values inhibition.

■ CONCLUSIONS

The objective of this work was to see the effect of noncovalent multinuclear platinum compounds upon condensation of DNA molecules. Our results show that these multinuclear platinum compounds are capable of inducing DNA condensation at more than 1 order of magnitude lower concentrations than conventional spermine. As expected from their higher charge of 6+, compounds **II** and **III** are more efficient in DNA condensation than **I**, suggesting that the major factor controlling DNA condensation is charge neutralization of negatively charged DNA phosphate groups. On the other hand, a marked difference between the efficiency of **II** and **III** having the same charge to condense DNA indicates that chemical structural differences of isovalent linear platinum cations may have a significant effect on the condensing effectiveness of this class of platinum compounds. We have shown that the DNA condensation by noncovalent analogues of polynuclear platinum complexes is a reversible process and that DNA can be released by a high concentration of monovalent cations. AFM studies of DNA condensation confined to a mica

dx.doi.org/10.1021/ic402796k | *Inorg. Chem.* 2014, 53, 1662−1671

substrate in the presence of noncovalent analogues of polynuclear platinum complexes have revealed that the DNA morphologies become more compact with increasing concentration of the platinum complexes. The higher concentrations lead to the formation of rather flat and single-layered compact DNA patterns on a mica surface. The results from AFM are in good agreement with the previously obtained data, confirming the high potency of platinum compounds to condense DNA in comparison with spermine or spermidine. Compound **III** is the most efficient among the tested complexes. Results of the competitive binding studies using the fluorescent intercalator EtBr have shown that **III** exhibits higher binding affinities for various DNA than **II** and **I**.

Moreover, its binding affinity toward synthetic double-stranded DNA copolymer poly(dA-dT)$_2$ is higher than that toward poly(dG-dC)$_2$ or CT DNA, suggesting a binding preference for sequences rich in AT pairs. Thus, to contribute to the understanding of how the polynuclear platinum complexes bind noncovalently to DNA, which is the major target of antitumor effects of platinum complexes, and more specifically how these metallodrugs condense DNA, a DNase I footprinting experiment was performed. Indeed, we demonstrate for the first time that **III** binds to DNA in a sequence-dependent manner, namely, to A/T-rich sequences and A-tract regions. Given the high negative electrostatic potential that envelopes the minor groove of AT-rich regions in B-DNA,[39−41] it seems reasonable to suggest that electrostatic attraction between the cationic polynuclear platinum compounds and AT-rich regions in B-DNA may have a favorable effect on this sequence specificity. However, it must be borne in mind that other factors, besides the purely electrostatic one, may contribute to the interaction energy. The DNase I footprinting experiment also showed that **I**−**III** could protect at micromolar concentrations DNA from enzymatic cleavage by DNase I.

Taken together, our results reported here demonstrate that noncovalent multinuclear platinum compounds represent a new type of effective agents capable of condensing DNA. Their ability to condense DNA at ∼20-fold lower concentration than spermine along with their sequence-specific DNA binding suggests that antitumor and cytotoxic activities of these complexes might be a direct consequence of their interaction with DNA. Owing to the high cellular accumulation of multinuclear platinum complexes, it is possible that their mechanism of action is based on the competition with naturally occurring polyamines such as spermine, spermidine, and putrescine for intracellular binding sites, resulting in a disturbance of the correct binding of regulatory proteins, which might initiate the onset of apoptosis.

■ EXPERIMENTAL SECTION

Chemicals. The noncovalent platinum compounds (Figure 1) were prepared by published procedures.[3] CT DNA (42% G+C, mean molecular mass of ca. 20000 kDa) was prepared and characterized as described previously.[42,43] Plasmid pSP73 (2464 bp) was isolated according to standard procedures. Poly(dG-dC)$_2$ and poly(dA-dT)$_2$ were obtained from Amersham Pharmacia-Biotech (Piscataway, NJ) and were used without further purification. The polynucleotides were dissolved in 10 mM NaCl and kept frozen until the day of the experiment. The DNA concentrations (moles of bases per liter) of all polynucleotides were determined spectroscopically by using molar extinction coefficients at the maximum of the long-wavelength absorbance: poly(dA-dT)$_2$, ε_{262} = 6600 cm^{-1} mol^{-1} dm^3; poly(dG-dC)$_2$, ε_{254} = 8400 cm^{-1} mol^{-1} dm^3; CT DNA, ε_{258} = 6600 cm^{-1} mol^{-1} dm^3. The Klenow fragment from DNA polymerase I (exonuclease minus, mutated to remove the 3′ → 5′ proofreading domain; KF$^-$), T4 polynucleotide kinase, and *Nde* I and *Hind* III restriction endonucleases were purchased from New England Biolabs (Beverly, MA). Deoxyribonucleoside 5′-triphosphates were from Roche Diagnostics GmbH (Mannheim, Germany). Acrylamide, bis-(acrylamide), urea, and ethidium bromide (EtBr) were from Merck KgaA (Darmstadt, Germany). Dimethyl sulfate, $MgCl_2$, 2-[4-(2-hydroxyethyl)-1-piperazinyl]ethanesulfonic acid (HEPES), spermine, spermidine, and sodium cacodylate were from Sigma (Prague, Czech Republic). [γ-^{32}P]-ATP was from MP Biomedicals, LLC (Irvine, CA). ATP was from Boehringer (Mannheim, Germany). Agarose was from FMC BioProducts (Rockland, ME). The Wizard SV and PCR cleanup system used to extract and purify the 158 bp DNA fragment (vide infra) was purchased from Promega. Deoxyribonuclease I (DNaseI) was from Roche (Mannheim, Germany).

Total Intensity Light Scattering. Light scattering experiments were performed using conditions similar to those described by Vijayanathan et al.[21] The experiments were carried out in a 10 mM cacodylade buffer, pH 7.2, at 25 °C. All buffers and stock solutions of condensing agents were filtered through 0.2 μm filters before use to avoid interference from dust particles. A 1.5 μM solution of CT DNA was prepared in a 1 cm quartz cuvette in a total volume of 2.5 mL. Small volumes (<10 μL) of condensing agents were added to the CT DNA solution to obtain the desired concentration, and the solution was thoroughly mixed by pipetting. The mixture was kept undisturbed for 20 min at room temperature. Total intensity light scattering was measured by using a Varian Cary Eclipse spectrofluorophotometer. The excitation and emission wavelengths were set to 305 nm, the excitation and emission slit widths were 5 nm, and the integration time was set to 5 s. The scattered light was measured at a 90° angle with respect to the incident beam. Statistical evaluation of the differences between the EC_{50} values determined for spermidine or spermine and the polynuclear platinum complexes was carried out using a Student's *t* test. If not stated otherwise, a probability of 0.005 or less was deemed statistically significant.

Gel Retardation Assay. Negatively supercoiled plasmid DNA pSP73 (10 ng μL^{-1}) was treated with the platinum compounds in a Tris-HCl buffer (10 mM, pH 7.4) with a total volume of 10 μL. After incubation for 20 min at 25 °C, 1.2 μL of loading dye (0.25% bromophenol blue and 60% glycerol) was added to the mixtures, and the samples were separated by electrophoresis on 0.8% native agarose gel running at 25 °C with a 0.5TAE (tris-aceate/EDTA) buffer for 120 min and the voltage set at 40 V. The gels were then stained with EtBr, followed by photography with a transilluminator.

Reversibility of DNA Condensation. The reversibility of DNA condensation induced by the platinum complexes was investigated by agarose gel electrophoresis. Plasmid pSP73 (10 ng μL^{-1}) was first treated with the platinum compounds (12.5 μM) in a Tris-HCl buffer (10 mM, pH 7.4). After incubation for 20 min at 25 °C, NaCl (0.65 M) was added to the mixtures, and the samples were analyzed by electrophoresis at the same conditions as those described in the preceding paragraph.

AFM Imaging. The plasmid pSP73 (2464 bp) was linearized by digestion with *Nde* I restriction endonuclease and purified using a Promega Wizard SV Gel cleanup system. The 158 bp fragment was prepared by digestion of supercoiled pSP73 plasmid with *Hind* III and *Nde* I restriction endonucleases to yield the 158 and 2306 bp fragments. The 158 bp fragment was then purified by 1% agarose gel electrophoresis and isolated from the gel by a Promega Wizard SV Gel cleanup system. Platinum complexes were dissolved in Milli-Q water (Millipore System, Billerica, MA), mixed with DNA (20 ng for linearized pSP73 or 5 ng for the 158 bp fragment) in 10 μL to obtain the desired concentration in the buffer containing 4 mM HEPES (pH 7.4), 5 mM KCl, and 5 mM $MgCl_2$, and incubated for 10 min at 25 °C. A droplet (4 μL) of the sample was spotted directly onto freshly cleaved mica (SPI, West Chester, PA). After 2 min of incubation, the mica was gently rinsed with 1 mL of Milli-Q water and immediately blown dry with compressed air. Imaging was performed using a MultiMode 8 atomic force microscope (Bruker, Santa Barbara, CA). Scanning was carried out in the tapping mode using 125 μm silicon

dx.doi.org/10.1021/ic402796k | Inorg. Chem. 2014, 53, 1662−1671

cantilevers with resonance frequencies of ~300 kHz (NT-MDT; Zelenograd, Moscow, Russia).

EtBr Displacement. The competition assays were all undertaken with fixed DNA and competitor (EtBr) concentrations and a variable platinum complex at 25 °C. Fluorescence measurements were performed on a Varian Cary Eclipse spectrofluorophotometer using a 0.5 cm quartz cell at room temperature. The DNA−EtBr complexes were excited at 546 nm, and the fluorescence was measured at 595 nm. To the solution of EtBr and DNA (10 mM Tris, pH 7.4, 1 mM EDTA, 1.3 mM EtBr, and 3.9 mM DNA) were added aliquots of a 1 mM stock solution of the platinum compounds, and the fluorescence was measured after each addition until the fluorescence was reduced to 50%. In general, the experiments were designed so that the weaker binder was displaced by the stronger one. The apparent binding constants (K_{app}) for both enantiomers were calculated from $K_{EB}[EB] = K_{app}[drug]$, where [EB] is the concentration of EtBr (1.3 mM), [drug] is the concentration of the platinum complexes at a 50% reduction of fluorescence, and K_{EB} is known [$K_{EB} = 1 \times 10^7$ M^{-1} for CT DNA; 9.5×10^6 M^{-1} for poly(dA-dT)$_2$, and 9.9×10^6 M^{-1} for poly(dG-dC)$_2$].[36]

DNase I Footprinting. Supercoiled pSP73 plasmid was digested with *Hind* III restriction endonuclease and 3′-end-labeled by treatment with Klenow exo$^-$ and [α-^{32}P]-deoxy-ATP. After radioactive labeling, the DNA first cleaved with *Hind* III was still digested with *Nde* I to yield 158 and 2306 bp fragments. The 158 bp fragment was purified by 1% agarose gel electrophoresis and isolated from the gel by a Promega Wizard SV Gel cleanup system.

A 9 μL solution containing a 1.11TKMC buffer (10 mM Tris, pH 7.9, 10 mM KCl, 10 mM $MgCl_2$, and 5 mM $CaCl_2$), 4.5×10^{-4} M DNA, and the platinum complex was incubated for 15 min at 25 °C. Cleavage was initiated by the addition of 1 μL of 50 μg mL^{-1} DNase I and allowed to react for 30 s at 25 °C before quenching with 2.5 μL of a DNase stop solution (3 M NH_4OAc and 0.25 M EDTA). This was then precipitated with ethanol, lyophilized, and resuspended in a formamide loading buffer. DNA cleavage products were resolved by poly(acrylamide) (PAA) gel electrophoresis under denaturing conditions (8%/8 M urea PAA gel). The autoradiograms were visualized and quantified by using a bioimaging analyzer. Assignment of the cleavage to a particular base has been made so that it corresponds to cleavage of the phosphodiesteric bond on the 5′ side of that base.

Flow LD. Flow LD spectra were collected using a flow Couette cell in a Jasco J-720 spectropolarimeter adapted for LD measurements. Long molecules, such as DNA (minimum length of ~250 bp), can be oriented in a flow Couette cell. The flow cell consists of a fixed outer cylinder and a rotating solid quartz inner cylinder, separated by a gap of 0.5 mm, giving a total path length of 1 mm. LD spectra of CT DNA at a concentration of 2×10^{-4} M were recorded at 25 °C in NaCl (10 mM) and sodium cacodylate (1 mM, pH 7.0).[44,45]

Other Physical Methods. Absorption spectra were measured with a Varian Cary 4000 UV/vis spectrophotometer equipped with a thermoelectrically controlled cell holder and quartz cells with a path length of 1 cm. The gels were visualized using a BAS 2500 Fujifilm bioimaging analyzer, and the radioactivities associated with the bands were quantitated with *AIDA* image analyzer software (Raytest, Germany).

■ ASSOCIATED CONTENT

Ⓢ Supporting Information

Representative AFM images of linearized plasmid pSP73 in the presence of spermidine and spermine and absorption spectra of CT DNA in the presence of complexes **I**−**III**. This material is available free of charge via the Internet at http://pubs.acs.org.

■ AUTHOR INFORMATION

Corresponding Author

*E-mail: brabec@ibp.cz.

Notes

The authors declare no competing financial interest.

■ ACKNOWLEDGMENTS

This work was supported by the Czech Science Foundation (Grant 13-08273S) and Ministry of Education of the CR (Grant LH13096).

■ REFERENCES

(1) Bloomfield, V. A. *Biopolymers* **1997**, *44*, 269−282.
(2) Teif, V. B.; Bohinc, K. *Prog. Biophys. Mol. Biol.* **2011**, *105*, 208−222.
(3) Qu, Y.; Harris, A.; Hegmans, A.; Petz, A.; Kabolizadeh, P.; Penazova, H.; Farrell, N. *J. Inorg. Biochem.* **2004**, *98*, 1591−1598.
(4) Farrell, N. Polynuclear platinum drugs. In *Metal Ions in Biological Systems*, Sigel, A., Sigel, H., Eds.; Marcel Dekker, Inc.: New York, 2004; Vol. *42*, pp 251−296.
(5) Mangrum, J. B.; Farrell, N. P. *Chem. Commun.* **2010**, *46*, 6640−6650.
(6) Gourley, C.; Cassidy, J.; Edwards, C.; Samuel, L.; Bisset, D.; Camboni, G.; Young, A.; Boyle, D.; Jodrell, D. *Cancer Chemother. Pharmacol.* **2004**, *53*, 95−101.
(7) Jodrell, D. I.; Evans, T. R. J.; Steward, W.; Cameron, D.; Prendiville, J.; Aschele, C.; Noberasco, C.; Lind, M.; Carmichael, J.; Dobbs, N.; Camboni, G.; Gatti, B.; De Braud, F. *Eur. J. Cancer* **2004**, *40*, 1872−1877.
(8) Hensing, T. A.; Hanna, N. H.; Gillenwater, H. H.; Camboni, M. G.; Allievi, C.; Socinski, M. A. *Anti-Cancer Drugs* **2006**, *17*, 697−704.
(9) Banerjee, T.; Dubey, P.; Mukhopadhyay, R. *Biochimie* **2010**, *92*, 846−851.
(10) Rauter, H.; Di Domenico, R.; Menta, E.; Oliva, A.; Qu, Y.; Farrell, N. *Inorg. Chem.* **1997**, *36*, 3919−3927.
(11) Farrell, N. Polynuclear charged platinum compounds as a new class of anticancer agents: Toward a new paradigm. In *Platinum-based Drugs in Cancer Therapy*; Kelland, L. R., Farrell, N. P., Eds.; Humana Press Inc.: Totowa, NJ, 2000; pp 321−338.
(12) Cox, J. W.; Berners-Price, S.; Davies, M. S.; Qu, Y.; Farrell, N. *J. Am. Chem. Soc.* **2001**, *123*, 1316−1326.
(13) Qu, Y.; Scarsdale, N. J.; Tran, M. C.; Farrell, N. P. *J. Biol. Inorg. Chem.* **2003**, *8*, 19−28.
(14) Hegmans, A.; Berners-Price, S. J.; Davies, M. S.; Thomas, D.; Humphreys, A.; Farrell, N. *J. Am. Chem. Soc.* **2004**, *126*, 2166−2180.
(15) Malina, J.; Farrell, N. P.; Brabec, V. *Chem.—Asian J.* **2011**, *6*, 1566−1574.
(16) Widom, J.; Baldwin, R. L. *J. Mol. Biol.* **1980**, *144*, 431−453.
(17) Harris, A. L.; Yang, X.; Hegmans, A.; Povirk, L.; Ryan, J. J.; Kelland, L.; Farrell, N. P. *Inorg. Chem.* **2005**, *44*, 9598−9600.
(18) Harris, A. L.; Ryan, J. J.; Farrell, N. *Mol. Pharmacol.* **2006**, *69*, 666−672.
(19) Carruthers, L. M.; Marton, L. J.; Peterson, C. L. *Biochem. J.* **2007**, *405*, 541−545.
(20) Valasinas, A.; Reddy, V. K.; Blokhin, A. V.; Basu, H. S.; Bhattacharya, S.; Sarkar, A.; Marton, L. J.; Frydman, B. *Bioorg. Med. Chem.* **2003**, *11*, 4121−4131.
(21) Vijayanathan, V.; Thomas, T.; Shirahata, A.; Thomas, T. J. *Biochemistry* **2001**, *40*, 13644−13651.
(22) Vijayanathan, V.; Lyall, J.; Thomas, T.; Shirahata, A.; Thomas, T. J. *Biomacromolecules* **2005**, *6*, 1097−1103.
(23) Zinchenko, A. A.; Sergeyev, V. G.; Yamabe, K.; Murata, S.; Yoshikawa, K. *ChemBioChem* **2004**, *5*, 360−368.
(24) Komeda, S.; Moulaei, T.; Chikuma, M.; Odani, A.; Kipping, R.; Farrell, N. P.; Williams, L. D. *Nucleic Acids Res.* **2011**, *39*, 325−336.
(25) Komeda, S.; Moulaei, T.; Woods, K. K.; Chikuma, M.; Farrell, N. P.; Williams, L. D. *J. Am. Chem. Soc.* **2006**, *128*, 16092−16103.
(26) Fant, K.; Esbjorner, E. K.; Lincoln, P.; Norden, B. *Biochemistry* **2008**, *47*, 1732−1740.
(27) Svensson, F. R.; Andersson, J.; Amand, H. L.; Lincoln, P. *J. Biol. Inorg. Chem.* **2012**, *17*, 565−571.
(28) Kankia, B. I.; Buckin, V.; Bloomfield, V. A. *Nucleic Acids Res.* **2001**, *29*, 2795−2801.

(29) Roy, K. B.; Antony, T.; Saxena, A.; Bohidar, H. B. *J. Phys. Chem. B* **1999**, *103*, 5117−5121.
(30) Perales, J. C.; Grossmann, G. A.; Molas, M.; Liu, G.; Ferkol, T.; Harpst, J.; Oda, H.; Hanson, R. W. *J. Biol. Chem.* **1997**, *272*, 7398−7407.
(31) Yan, H.; Li, Z.-F.; Guo, Z.-F.; Lu, Z.-L.; Wang, F.; Wu, L.-Z. *Bioorg. Med. Chem.* **2012**, *20*, 801−808.
(32) Dong, X.; Wang, X.; He, Y.; Yu, Z.; Lin, M.; Zhang, C.; Wang, J.; Song, Y.; Zhang, Y.; Liu, Z.; Li, Y.; Guo, Z. *Chem.—Eur. J.* **2010**, *16*, 14181−14189.
(33) Sun, S.; Liu, W.; Cheng, N.; Zhang, B.; Cao, Z.; Yao, K.; Liang, D.; Zuo, A.; Guo, G.; Zhang, J. *Bioconjugate Chem.* **2005**, *16*, 972−980.
(34) Hibino, K.; Yoshikawa, Y.; Murata, S.; Saito, T.; Zinchenko, A. A.; Yoshikawa, K. *Chem. Phys. Lett.* **2006**, *426*, 405−409.
(35) Fang, Y.; Hoh, J. H. *J. Am. Chem. Soc.* **1998**, *120*, 8903−8909.
(36) Wyatt, M. D.; Garbiras, B. J.; Haskell, M. K.; Lee, M.; Souhami, R. L.; Hartley, J. A. *Anti-Cancer Drug Des.* **1994**, *1*, 511−529.
(37) Fairall, L.; Rhodes, D. *Nucleic Acids Res.* **1992**, *20*, 4727−4731.
(38) Lindemose, S.; Nielsen, P. E.; Mollegaard, N. E. *Nucleic Acids Res.* **2005**, *33*, 1790−1803.
(39) Pullman, B.; Lavery, R.; Pullman, A. *Eur. J. Biochem.* **1982**, *124*, 229−238.
(40) Nielsen, P. E.; Mollegaard, N. E.; Jeppesen, C. *Nucleic Acids Res.* **1990**, *18*, 3847−3851.
(41) Lindemose, S.; Nielsen, P. E.; Hansen, M.; Mollegaard, N. E. *Nucleic Acids Res.* **2011**, *39*, 6269−6276.
(42) Brabec, V.; Palecek, E. *Biophysik* **1970**, *6*, 290−300.
(43) Brabec, V.; Palecek, E. *Biophys. Chem.* **1976**, *4*, 76−92.
(44) Rodger, A. *Methods Enzymol.* **1993**, *226*, 232−258.
(45) Rodger, A.; Norden, B. *Circular Dichroism and Linear Dichroism*; Oxford University Press: Oxford, U.K., 1997.